

## UNDERGROUND GASIFICATION OF COAL: THE FILLING OF DIPPING UNDERGROUND CAVITIES<sup>1</sup>

A. W. GRUPPING<sup>2</sup> & R. PIETERSON<sup>2</sup>

### ABSTRACT

Gruppings, A. W. & R. Pieterse 1980 Underground gasification of coal: the filling of dipping underground cavities – Geol. Mijnbouw 59: 289-299.

In deep underground coal gasification the all-important parameter is the volume of coal that can be gasified between two boreholes. This volume depends to a large extent on the maximum attainable linking distance.

Spectacular advances in recent years in deviated drilling techniques suggest that the linking of deep boreholes can more easily be achieved by drilling than by conventional methods such as fracturing. Gasification methods could then be developed in dipping coal seams in which the combustion front is, from time to time, driven updip by backward filling of the cavity with a filler such as sand.

The results of filling tests in a scaled model are described. It is shown that dipping underground cavities can be completely filled by a process of sedimentation, with the exception of an updip channel along the coal face. Through this channel combustion can be re-initiated after removing the excess water with high-pressure gas. In this way a number of roughly parallel strips of coal could be gasified between two boreholes; serious subsidence at the surface would then be avoided.

The tests also show that localized caving-in of the roof of the cavity does not seriously disturb the filling process or the development of the updip channel.

### INTRODUCTION

In recent years the looming shortages of oil and natural gas have generated much interest in the development of alternative sources of energy. Of these the potential coal reserves underlying Western Europe and the U.S.A. are very large and increasing attention is being paid to the possibilities of exploiting this type of coal with unconventional methods.

Underground gasification of coal (UGC) is one of such methods. In Russia, UGC processes have been under development since the 1930's. They are now being commercially applied at shallow depth and on a small scale. In other countries activity is increasing and a number of UGC pilot tests are now underway or in the planning stage, notably in the U.S.A., Canada and Belgium/Germany.

In The Netherlands, there has never been much interest in underground gasification of coal. The Dutch coal reserves are located at great depth and their exploitation by UGC methods was rightly felt not to be technically and economically feasible, even at the greatly increased energy prices.

The main reason for this was the limited linking distance between two wells. This distance determines the length of the burnt-away cavity; with available linking techniques, such as hydraulic fracturing, it is no more than, say, 20-30 metres. In thin layers this limits the amount of coal that can be gasified between two holes to a few thousand tons. With current drilling costs, this makes the process only economical at very shallow depth.

However, spectacular advances in deviated and horizontal drilling techniques have been made in recent years. For instance, it is now possible to deviate holes from the surface into a 1.80 m thick coal layer at a depth of 300 m over distances of 900 m in less than two weeks (NESVACIL, 1980). These developments suggest that in future the linking of boreholes in deep coal seams will be carried out by drilling instead of fracturing; this would considerably increase the linking distance and thus the volume of coal that can be gasified between boreholes.

Further increases could be obtained by periodically back-filling the burnt-out cavity with a filler. Gasification methods employing backfills can only be used in dipping coal seams. They can be carried out with several different borehole configurations. A basic requirement is that an updip channel, through which the combustion process can be restarted, re-

<sup>1</sup> Manuscript received: 1980-03-27.

Revised manuscript received and accepted: 1980-07-28.

<sup>2</sup> Delft University of Technology, Mining Faculty, Mijnbouwstraat 120, DELFT, The Netherlands.

Table I  
List of symbols (units: Standard International, M.K.S.).

A	= cross-sectional area of channel	
a	= constant, connected with the transport mechanism	
b	= subscript: boundary	
c	= subscript: channel	
Cd	= drag coefficient	
Cs	= concentration of sand in suspension	
D	= hydraulic diameter of chamber	
d	= diameter of grain	
f	= subscript: field	
Fr	= Froude number	
g	= acceleration of gravity	
g	= subscript: grain	
h	= height of channel	
m	= subscript: model	
n	= linear scale factor	
P	= pressure	
Q	= throughput	
R	= resistance	
Re	= Reynolds number	
S	= sedimentation constant	
s	= ratio density grains/liquid	
T	= time	
V	= axial velocity in chamber	
V <sub>o</sub>	= sedimentation velocity of grain	
w	= width of the channel	
x y z	} = three directions in the co-ordinate system	
α		= dip angle of the model
Δ		= difference (of pressure P)
η	= viscosity	
ρ	= density	

mains open along the face of the coal seam.

A system employing two boreholes, both deviated along a coal seam in a downdip direction, has been described in detail in a paper in Dutch language (GRUPPING, 1978).

The idea of filling gasification voids in dipping coal seams is not new. Russian trials, carried out with dry fillers and slurries, proved to be unsatisfactory because the distribution of the fill was spotty and the filling material did not reach the desired area's, owing to the peculiar pattern of burning (TYUTIN, 1958).

It was felt at Delft University that a better way of filling a gaschamber might be by a process of sedimentation, such as has been developed for tunnel foundation (GRIFFIOEN & VAN DER VEEN, 1972). The cavity is first completely filled with water, after which sand, suspended in water, is circulated into it through one of the holes. The sand settles out and fills the cavity gradually from this injection hole in the direction of

the discharge hole.

Based on the experiments carried out by GRIFFIOEN & VAN DER VEEN (1972) it was postulated that a channel would automatically remain open updip along the coal face through which gasification could be restarted after removal of the water from the cavity.

To investigate the merits of this filling mechanism, a number of experiments was carried out in a transparent model, scaled 1 to 20. It was found that the filling of the cavity and the formation of the channel are both possible under a wide range of operating conditions. It was also found that fairly small simulated caved-in sections of the roof have no influence on the filling process and the development of the channel.

## EXPERIMENTAL WORK

### Scaling rules

To carry out model tests that are representative for field conditions, scaling rules had to be established. For a list of symbols, reference is made to table I.

The following parameters are relevant: the Reynolds number, the Froude number, the density ratio grains/liquid, the coefficients of friction and restitution and the geometrical relationships (shape and size distribution of grains, the relation of grain diameter to hydraulic diameter of the model, the grain concentration).

The model was scaled 1 to 20 and a suspension of sand in water was used. It is not possible to satisfy all the scaling rules simultaneously; a choice needs to be made between equality of the Reynolds number, the Froude number or a combination of these numbers.

An analysis of the grain transport mechanism showed that the most important requirement was to keep constant the ratio between the mean settling velocity of the grains and the axial liquid velocity in the chamber.

$$S = \frac{V_o}{V}; S_m = S_f$$

It was also established that the Reynolds number is of minor importance in this type of transport process.

The ratio between the grain diameter and the hydraulic diameter of the chamber is also of secondary importance; this ratio is very small, both in the model and in the field.

Since the Froude number is a measure of the inertia effects that act on the grains and thus influences the movement and transportation of the grains, it was decided to keep this number the same in model and field. For the model this results in reasonable grain sizes and injection velocities. This second requirement can be formulated as follows:

$$Fr_m = Fr_f; \frac{V_m^2}{g \cdot D_m} = \frac{V_f^2}{g \cdot D_f}$$

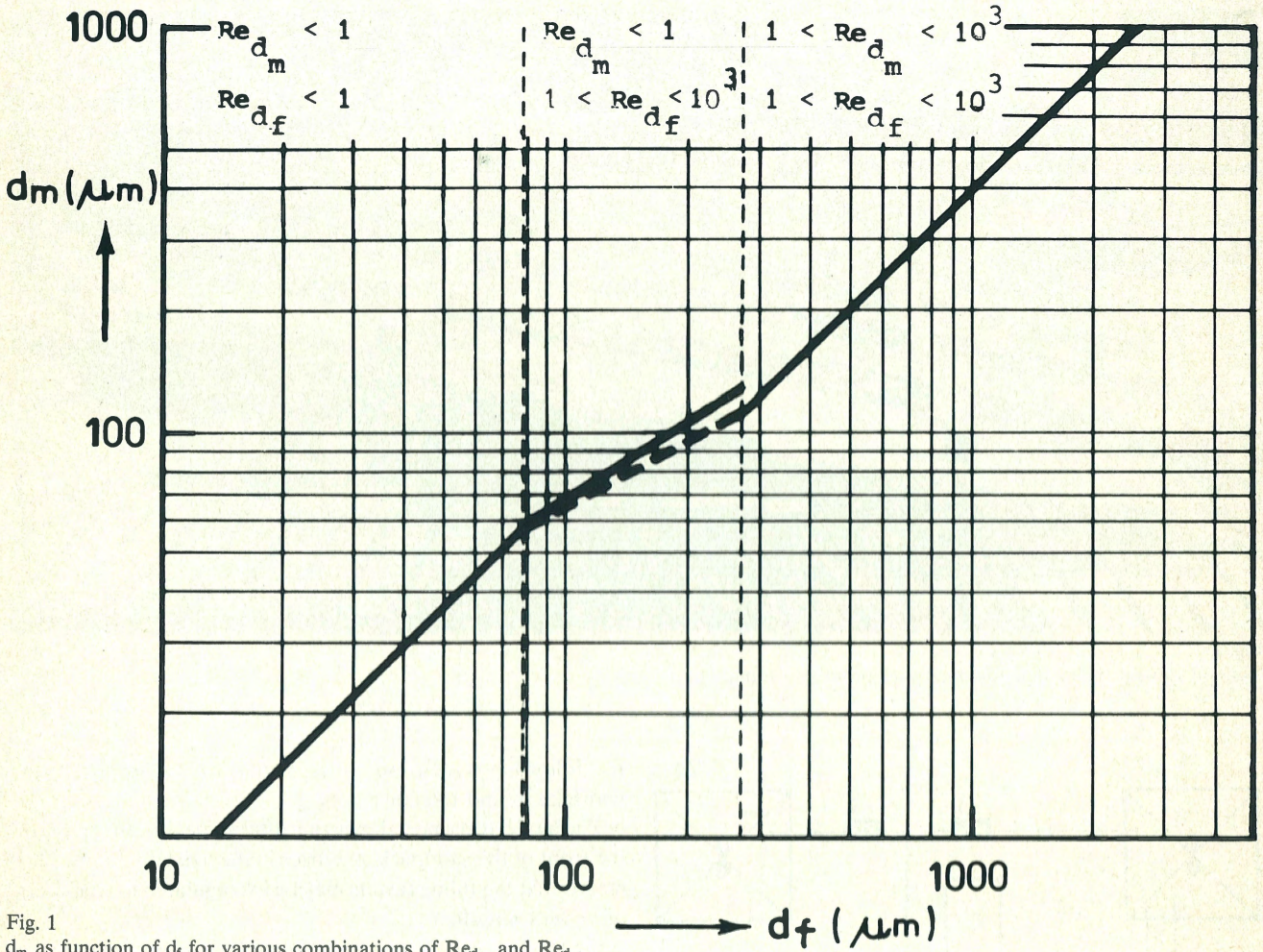


Fig. 1  
 $d_m$  as function of  $d_f$  for various combinations of  $Re_{d_m}$  and  $Re_{d_f}$ .

This Froude number relates to the whole chamber; it can be shown that the Froude numbers for the transportation through what might be called the 'rivers' in model and field are also approximately equal.

The third requirement is that the dimensions in the x, y and z directions should be scaled down by a factor of 20:

$$20 \cdot (x, y, z)_m = (x, y, z)_f$$

The first requirement caused an adjustment of the grain size, the second an adjustment of the throughput. This has finally led to the following scaling rules for grain size, throughput, time and concentration:

(1) Grain size

There are three relationships between the grain diameter in the model and that in the field. These depend on the Reynolds number of the grains, which is defined as:

$$Re_g = \frac{\rho_g \cdot V_o \cdot d}{\eta}$$

In this equation  $\rho_g$  is the density of sand,  $d$  is the sand-grain diameter and  $\eta$  is the water viscosity.

With an assumed water temperature of 10 °C in the model and 55 °C in the field, the following relationships are valid if the linear scale factor is 20:

$Re_{g_m} < 1; Re_{g_f} < 1:$	$d_m = 0.76 d_f$
$Re_{g_m} < 1; 1 < Re_{g_f} < 1000:$	$d_m = 0.017 (d_f)^{0.6}$
$1 < Re_{g_m} < 1000; 1 < Re_{g_f} < 1000:$	$d_m = 0.41 d_f$

Figure 1 shows the relationship between  $d_m$  and  $d_f$  for the three domains. A small adjustment had to be made in the middle area to match the endpoints of the lines.

(2) Throughput  $Q_m = 0.00056 Q_f$

(3) Time  $T_m = 0.22 T_f$

(4) Concentration  $C_{s_m} = C_{s_f}$

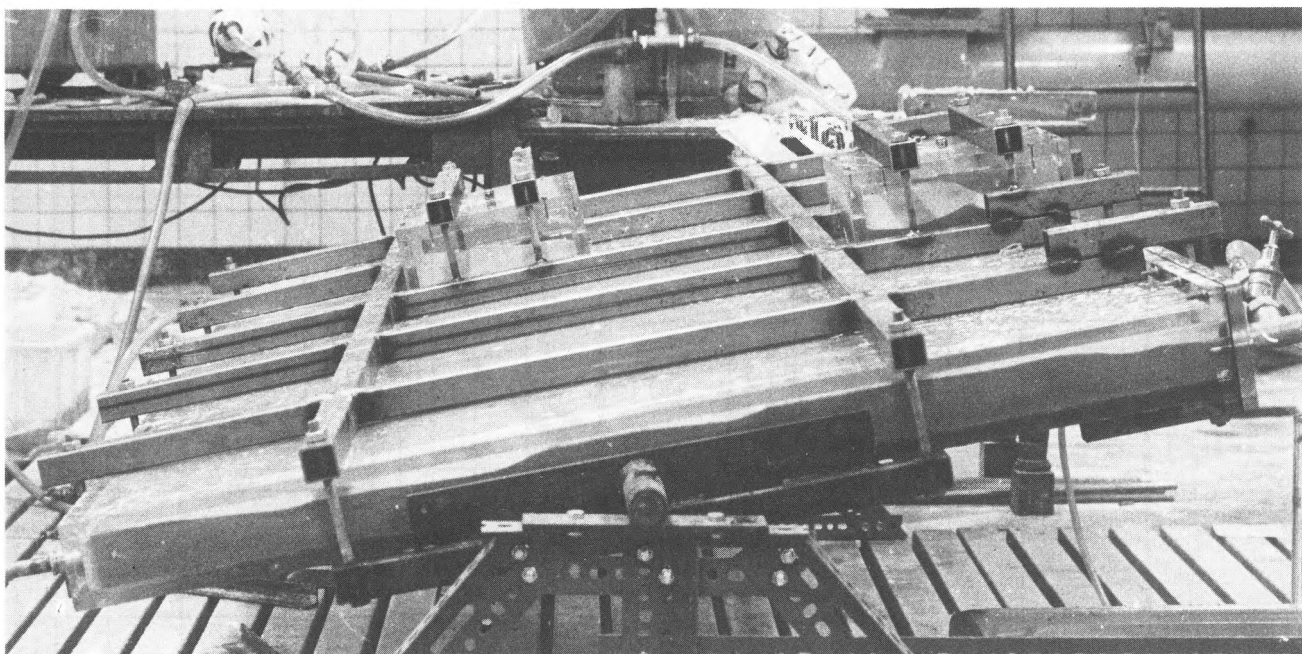


Fig. 2  
General view of the model, equipped with protective frame.

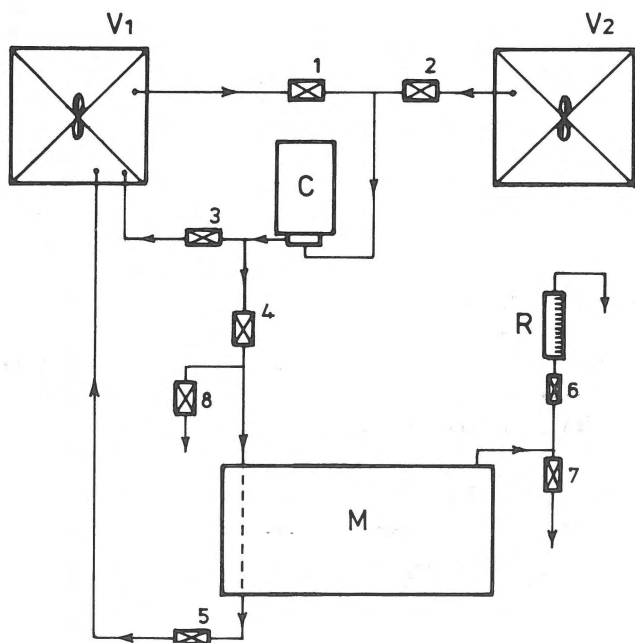


Fig. 3  
The suspension supply system.  
V1, V2 = mixing containers; C = centrifugal pump; M = model;  
R = rota meter; X1-8 = valves.

### The model

The dimensions of the model are: length 2 m, width 1 m, and thickness 5 cm. With a scale factor  $n = 20$ , this corresponds to

the following dimensions of an actual cavity: length 40 m, width 20 m and thickness 1 m.

The model tests have shown that after some time the shape of the front of the sandpack stabilizes in the axial direction. This means that the filling results may be extrapolated to chambers of greater length.

Figure 2 shows the model which is built of perspex plates with a thickness of 1.5 cm. The floor plate is roughened to approximate field conditions as much as possible. The 'coal seam' consists of a front plate that can be detached to remove the sand from the model after each experiment. A steel frame protects the model against excessive internal pressures. The lower part of this frame rests with bearings on two supports. In this way the model can be adjusted to correspond to various dip angles. The water supply and circulation system is schematically shown in figure 3. The mixing containers are alternately used for filling the model.

Initially, problems occurred because of plugging in the injection lines. These were solved by creating a bypass via valve 5. In this way, the velocity of the suspension in the injection lines could be increased, without increasing the throughput of the model. The injection line passes through the model and carries part of the suspension back to the container V1. This configuration also acts as a safety valve, because an unexpected increase of pressure in the model automatically bleeds off through valve 5.

The suspension enters the model through one or more perforations in the injection line. The throughput is adjusted by the valves 6 or 7. The water leaves the model through a hole in the frontplate.

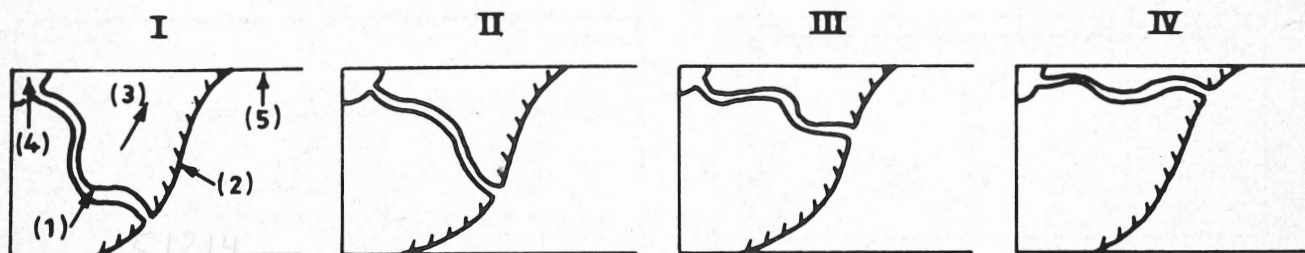


Fig. 4

Four stages of the sand transportation mechanism from the injection opening via the turning 'river'. (1) = meandering 'river'; (2) = front of the sand pack; (3) = direction in which the 'river' turns; (4) = crater; (5) = front plate.

### Experiments in the model

A total of seventeen experiments were carried out with the model. Sorted sands with a  $d_{50}$  of  $96 \mu\text{m}$  and  $133 \mu\text{m}$  were used. This corresponds to field grain sizes of  $210 \mu\text{m}$  and  $325 \mu\text{m}$  (see Fig. 1). The throughput varied from 2.8 litres per minute to 6 litres per minute. In the field this corresponds to a rate between  $5 \text{ m}^3/\text{minute}$  and  $10.7 \text{ m}^3/\text{minute}$ . The sand concentration  $C_s$  was kept constant at 5 percent by volume in all tests.

In most experiments one set of perforations was used, at the upper end of the injection tube. The discharge consisted in most cases of a hole in the front plate.

The amount of time each experiment takes depends on the throughput. At 3 litres/minute it is approximately 6 hours, which corresponds to slightly over 24 hours in practice when the chamber is 40 metres long.

To test the scaling rules, some experiments were carried out with an identical sedimentation constant  $S$ , but with different grain size  $d$  and different throughput  $Q$ . It was found

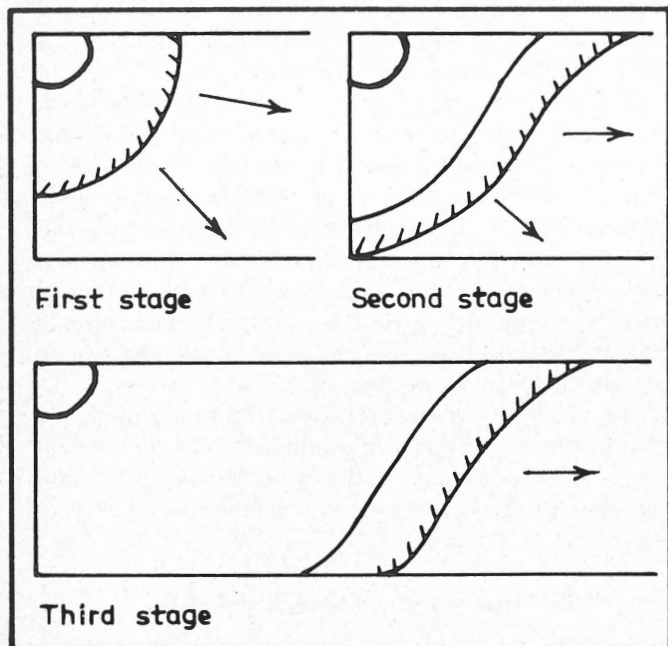


Fig. 5

Three stages of the filling process.

that in that case the sedimentation process is identical. Because  $Q$  was different, the Froude number was also different. Apparently the Froude number is of only minor importance in the sedimentation process.

### General description of the experiments

As soon as the suspension leaves a perforation, the velocity of the sand/water mixture decreases rapidly and sand settles out. A crater develops, of which the wall increases continuously in height as more and more sand settles out. Finally, the velocity of the suspension in the boundary layer between the sand pack and the top plate becomes sufficiently high to carry away sand grains that had been deposited earlier. What might be called a 'river' then develops in the sand pack, which rapidly grows to such a cross-sectional area that the pressure drop in it is minimal. This 'river' does not meander in arbitrary directions but gradually turns updip, towards the front plate, as indicated in figure 4. In the meantime, a rim of sand is deposited at the face of the sand pack.

When the 'river' has moved to the frontplate, it has become an updip channel. This channel is not stable; it silts up after it has transported sand for some time. A new 'river' then develops from the crater and the process repeats itself. Meanwhile, the face of the sand pack has moved forward. The filling process can be divided into three stages, as detailed in figure 5.

In the first stage the sand pack grows in circles from the original crater. Its radius is proportional to the square root of time. In the second stage the sand front gradually assumes an S-shape as a result of increasing influence of the channel transport. Finally the shape of the front does not change anymore and it propagates itself towards the end of the chamber proportionally with time.

When the sand front has reached the end of the chamber, a downdip corner of the chamber remains unfilled. This is because the front does not propagate itself perpendicularly to the channel but at an angle (see Fig. 5, third stage). This corner can easily be filled by locating the opening, through which the water leaves the model, downdip. The channel then follows the path as shown in figure 6.

The dip of the model, if not too big, has little or no influence on the filling process. With a dip of  $5^\circ$  the angle of the sand

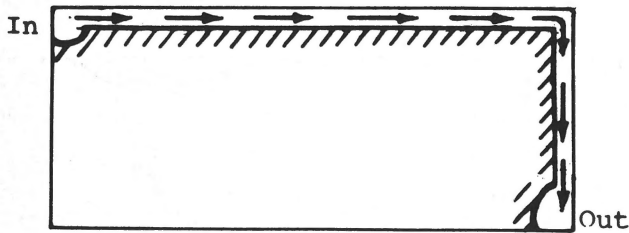


Fig. 6  
The path of the channel through the sand fill if the discharge opening is located downdip in the chamber.

front with the channel is about 50° and with a dip of 20° it is about 70°.

*Methods of sand transportation; the mechanism of filling*

- Two methods of sand transportation can be distinguished:  
 (1) suspension transportation through 'rivers' or through the channel;  
 (2) transportation of water with some fine sand through the boundary layer.

The interaction between these two types of transportation causes the periodic silting up and re-opening of the channel.

After some time, when the sand body has spread over the full width of the model, new 'rivers' do not originate from the original crater, but from a point in the channel. These 'rivers' also meander and turn upward and finally re-establish the channel. Three factors are important in this process of 'river'-forming: throughput, resistance and pressure difference. The following relationship exists for the transportation through the channel as well as through the boundary layer:

$$\Delta P = Q^a \cdot R$$

( $\Delta P$  = the pressure drop; the constant  $a$  is smaller than 0 for channel transportation and larger than 0 for boundary transportation).

Figure 7 shows the situation in a period that transportation takes place through the channel. Through the channel and across the boundary layer the same pressure drop exists. As the channel grows in length, the resistance through it increases and so does the pressure drop. Because the pressure drop

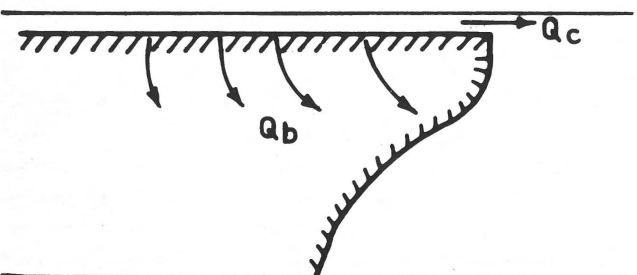


Fig. 7  
Transportation via the boundary layer, starting from the channel.  $Q_c$  = channel throughput;  $Q_b$  = boundary layer throughput.

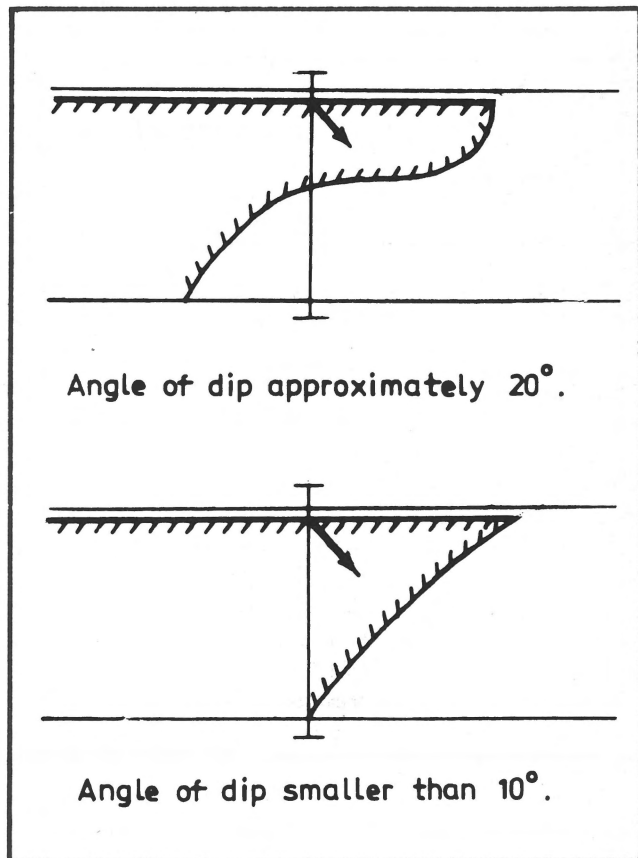


Fig. 8  
Types of 'river' development from the channel at different angles of dip of the model.

across the boundary layer also increases and the resistance of the boundary layer is practically constant, the throughput  $Q_b$  of the boundary layer must increase.

At a constant injection rate the sum of the throughputs through the channel and the boundary layer is constant. Therefore  $Q_c$  must decrease and because, in the case of channel transport ( $a < 0$ ), the pressure drop  $\Delta P$  increases further. Finally,  $Q_c$  has become so small that the channel silts up. The transportation through the boundary layer has now become very strong and a new 'river' develops, starting at some point in the channel. This 'river' again turns upward and, while doing so, deposits a new rim of sand. This process repeats itself over and over again.

The model experiments have shown that the point in the channel where new 'rivers' originate is different for different shapes of the sand front, depending on the angle of the model. Figure 8 shows two situations; however, these are not fundamentally different.

*The channel: pressure losses through the channel*

The shape of the channel is approximately as shown in figure 9. Its cross-section is such that the Froude number of the

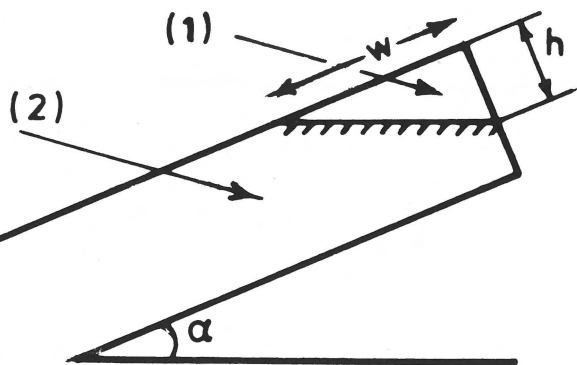


Fig. 9  
Shape of the channel.  
1 = channel; 2 = sand fill.

channel remains constant: the pressure drop through the channel is always minimal (GOVIER & AZIZ, 1972). This has been experimentally verified in the tests. From this follows the relationship between the throughput  $Q$  and the height  $h$  of the channel:

$$Q = \text{const}_1 \cdot h^{2.5}$$

This constant is dependent on the angle of the dip of the model. With this equation, the scaling rule for the cross-section  $A$  for field and model can also be deduced:

$$A_f/A_m = \text{const}_2 \cdot n^2$$

This second constant is dependent on the sand concentration, the specific density of sand and water and on the grain size.

Knowing that the cross-section of the 'rivers' and the channel is such that the pressure drop through them is minimal, this cross-section can be calculated:

$$A = 0.16 \cdot C_s^{-0.21} \cdot (s - 1)^{-0.4} \cdot C_d^{0.2} \cdot F(\alpha) \cdot Q^{0.8}$$

Table II presents values of  $F(\alpha)$  for various values of the dip angle  $\alpha$ . The table shows that  $\alpha$  has little influence on the cross-section of the channel.

To obtain a general impression of the magnitude of this cross-section in the model and in the field, it has been calculated for the following conditions:

Model: throughput =  $2.8 \times 10^{-3} \text{ m}^3/\text{min}$ ,  $d_{50} = 96 \mu\text{m}$ ,  $C_s = 5 \text{ vol.}\%$ ,  $\alpha = 20^\circ \rightarrow A_m = 1.35 \text{ cm}^2$ .

Field: throughput =  $5 \text{ m}^3/\text{min}$ ,  $d_{50} = 210 \mu\text{m}$ ,  $C_s = 5 \text{ vol.}\%$ ,  $\alpha = 20^\circ \rightarrow A_f = 840 \text{ cm}^2$ .

Table II  
Function  $F(\alpha)$  for various values of the dip angle  $\alpha$ .

$\alpha$	$F(\alpha)$
$5^\circ$	0.89
$10^\circ$	0.80
$15^\circ$	0.76
$20^\circ$	0.73

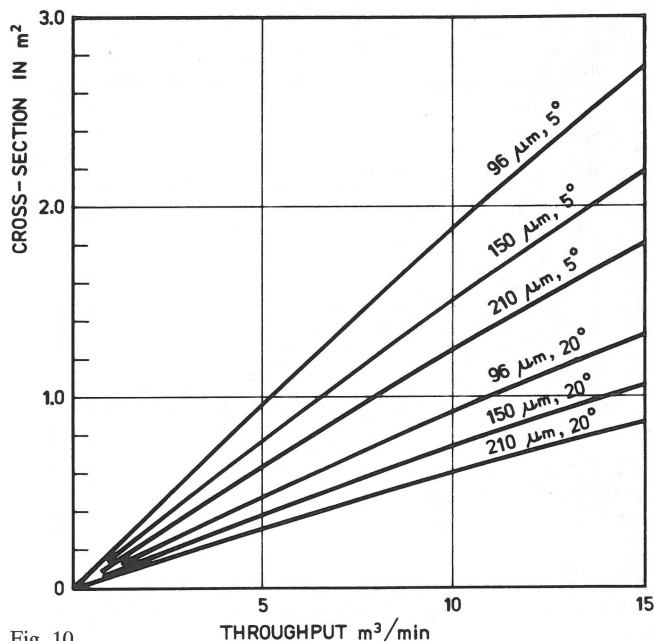


Fig. 10  
The relationship (after washing out with water) between the cross-section of the channel and the throughput for various grain sizes and dip angles – field conditions.

The calculated model value corresponds reasonably well with the measured value of  $1.20 \text{ cm}^2$  for the channel under these conditions.

#### *Increasing the cross-section of the channel by water circulation*

When the water is circulating, grains that have been deposited are carried away again, as a result of which the cross-section of the channel increases. Ultimately, a critical cross-sectional area is reached through which the velocity of the water is so low that transportation of deposited sand stops. A small increase of throughput at that point will result in renewed sand transportation.

This point (at which the sand begins to move again) is determined by the Shields criterion, which defines it by means of dimensionless numbers (YALIN, 1972). A detailed description of the Shields theory falls outside the scope of this paper. Suffice it to say that by the use of this criterion a relationship can be established with which the cross-section of the channel, after washing out with water, can be calculated.

Figure 10 shows the cross-section of the washed-out channel for field conditions as a function of the throughput. It is noteworthy that the dependence on the model dip  $\alpha$  is rather pronounced. It was also noted qualitatively that washing-out with mixtures of air and water further increases the cross-section.

Finally, it was observed that at certain throughputs sand waves develop in the channel both while injecting the suspension and while washing-out with water. The cross-section

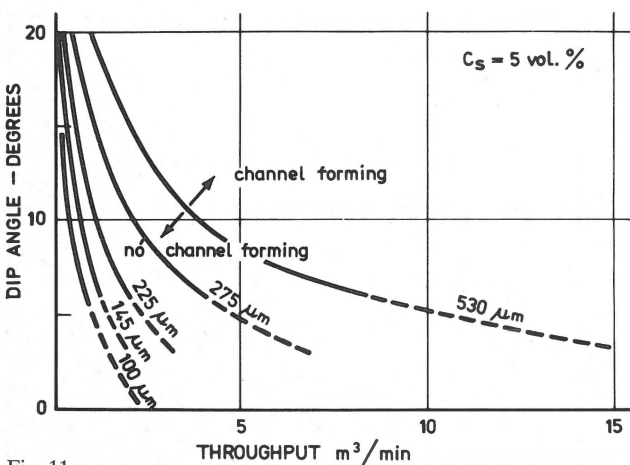


Fig. 11  
Development of the channel at various grain sizes, throughputs and dip angles – field conditions.

remains constant, however: in places where the height  $h$  of the channel is smaller, at the top of a wave, the width  $w$  of the channel is larger. In figure 2 these waves can clearly be seen in the channel that develops at the side of the model when the exit opening is located downdip.

#### Causes of dying-out of the filling process

Most of the transportation of water and sand takes place through the meandering 'rivers' and the channel. Some water, with fine sand, leaks away through the boundary layer. In addition, water is transported through the permeable sand pack, but this is relatively insignificant and has been neglected.

When the boundary layer is thick, more liquid is transported through it and, therefore, less is available for the 'rivers'. Above a certain critical thickness of the boundary layer the throughput of the 'rivers' becomes so small that they silt up and the process terminates gradually (with the exception of some remaining transportation through the boundary layer). This causes a pressure increase in the model and increased circulation through the bypass.

In the field under these circumstances, the injection pressure will also increase, after which the injection borehole will probably plug with sand. This critical point in the process is governed by three parameters: grain size, throughput and dip angle of the model. Empirically, relationships have been established in the model between these three parameters. These were then translated to field conditions. Figure 11 shows the critical dip angle  $\alpha$  as a function of the critical throughput for various grain sizes. It is clear that, at a constant value of the grain size, a sufficiently large increase of the throughput or the dip angle will re-activate the filling process.

In general, injection rates of  $10 \text{ m}^3/\text{minute}$  should be attainable in the field if the casing size is not too small. With an average grain size of  $530 \mu\text{m}$  it is then possible to fill cham-

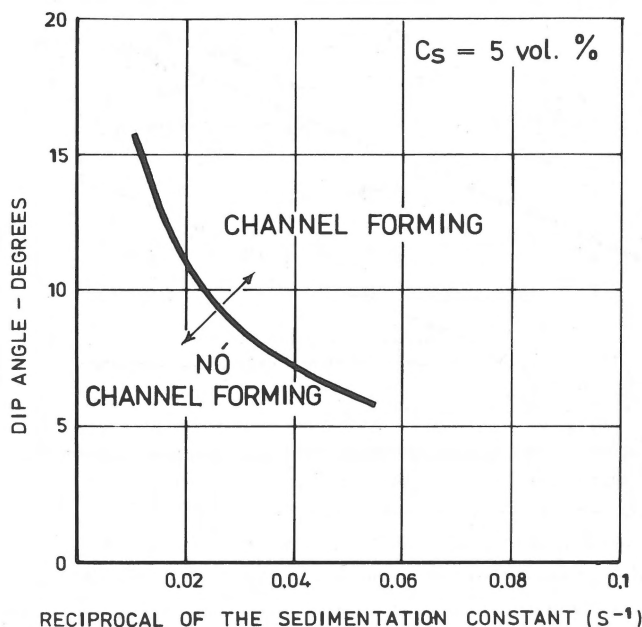


Fig. 12

Development of the channel at various values of the reciprocal of the sedimentation constant and dip angles – model and field conditions.

bers with a dip angle down to about  $6^\circ$ . In flatter seams the injection rate would have to be further increased or a smaller grain size would have to be selected.

Figure 11 can be transformed to figure 12, in which form it is applicable to both model and field conditions. For this, the horizontal scale must show the reciprocal of the sedimentation constant  $S$ . Because  $S$  is proportional to  $V_0/Q$ ,  $Q$  is proportional to  $V_0/S$ . Dividing by the  $V_0$ -values of the various grain sizes produces one curve that is universally valid.

It is very likely that the periodic alternation between 'river' transportation and boundary layer transportation has caused the strongly fluctuating water production rates of the breakthrough of water and sand in the Dutch coal mine Julia in Eyselshoven in 1958 (DE GROOT, 1958). These fluctuations have never been satisfactorily explained.

In this breakthrough the grain size of the sand was mainly in the range from  $80$  to  $120 \mu\text{m}$ . The water production rate was  $0.5$  to  $1.0 \text{ m}^3/\text{minute}$ , alternating with a rate of  $2.0$  to  $4.0 \text{ m}^3/\text{minute}$ , lasting from 30 minutes to one hour. The sand concentration averaged 9 to 10 percent by volume.

When extrapolating the  $100 \mu\text{m}$ -line of figure 11 to small dip angles it is seen that the change from 'river' transportation to boundary layer transportation occurs at throughputs of about  $2$  to  $2.5 \text{ m}^3/\text{minute}$ . Breakthroughs of water and sand have also occurred in other coal mines. A very serious one, which took place in the mine Sophia-Jacoba in Germany in 1975, was described by SOMMER (1977).

#### The influence of injection and discharge point on the filling process

If injection of the suspension takes place through a number

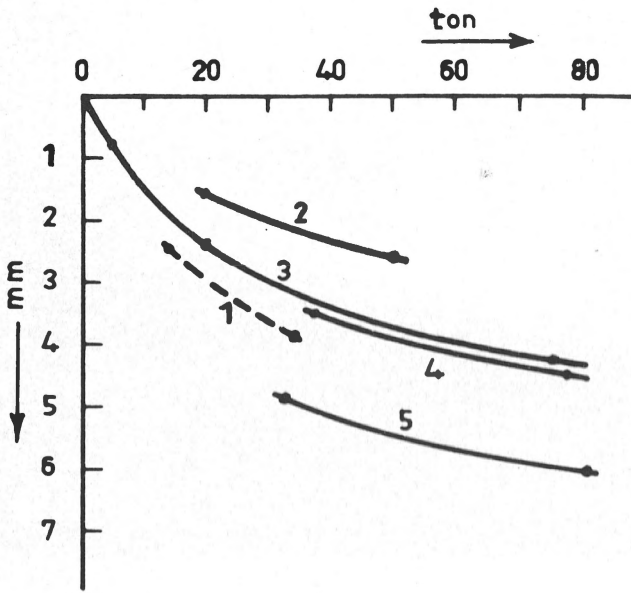


Fig. 13  
Compression as a function of the load (per 100 m<sup>2</sup>).  
1 = Plate sand, thickness 20 cm, throughput 1.2 m<sup>3</sup>/min; 2 = Zealand sand, thickness 20 cm, throughput 1.2 m<sup>3</sup>/min; 3 = Zealand sand, thickness 70 cm, throughput 1.2 m<sup>3</sup>/min; 4 = Zealand sand, thickness 60 cm, throughput 3.6 m<sup>3</sup>/min; 5 = Zealand sand, thickness 60 cm, throughput 4.8 m<sup>3</sup>/min.

of perforations along the dip of the model, a crater develops at each perforation. After some time the streams from the craters collect into one stream, which moves vertically upward along the dip towards the front plate. Thereafter, the system behaves as if there were one opening, directly beneath the front plate.

With only one perforation at the bottom, an identical situation is created. Initially, the sand wall extends in a circular manner around the opening. After some time, the suspension flows from the crater near the bottom vertically upward along the dip after which the system again behaves as if the injection point were directly beneath the front plate.

If the discharge consists of one updip perforation, an unfilled space remains downdip in the model, as described earlier. With the discharge at the bottom, this empty space is eliminated and the chamber fills completely. The point of injection therefore has no essential function in the filling process. Locating the discharge point at the lower end eliminates the empty space downdip.

#### Functions and quality of the sand fill

The two most important functions of the fill are: (1) to narrow the gaschamber periodically so that gasification can be resumed in a turbulent environment; and (2) to support the roof to counter the tendency of it to cave in.

No measurements have been made to check the quality of the sand fill in the model. Visual inspection invariably showed that the model – except for the channel and the ‘end’ effect – was completely filled with a dense sand pack. Small

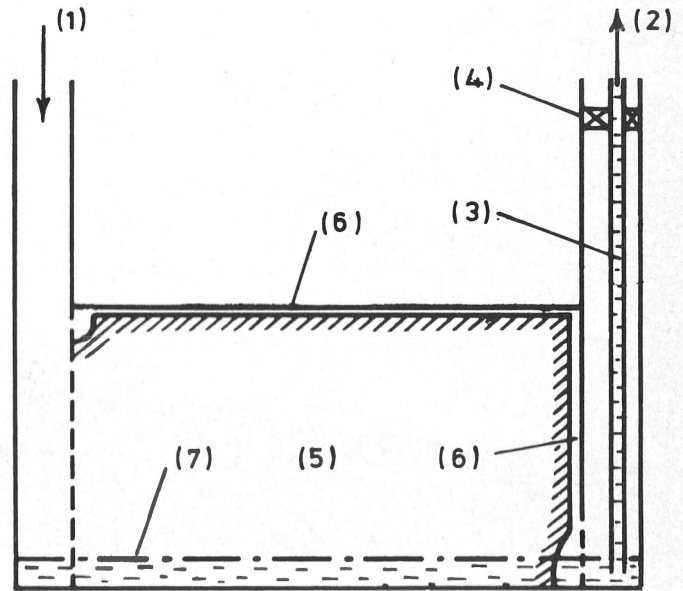


Fig. 14  
Dewatering of the sand fill with compressed air and tubing (supply openings distributed over the width of the model, discharge opening at the bottom).  
(1) = compressed air; (2) = produced water; (3) = tubing; (4) = packer; (5) = sand fill; (6) = channel; (7) = liquid level.

cavities and openings that remained after the sand front had passed, always filled up completely by particle transport via the boundary layer. In one experiment the porosity could be determined with reasonable accuracy from the speed of propagation of the sand front at known injection rate and sand concentration. For the grain size of 96  $\mu\text{m}$  the porosity was found to be 44%. This value corresponds well with values found in similar sedimentation tests in horizontal chambers (GRIFFIOEN & VAN DER VEEN, 1972). Therefore, there appears to be no reason why the compression under loading of fills in dipping chambers should be significantly different from that in horizontal ones. Figure 13 gives the results of past compression tests on various types of sand fill (GRIFFIOEN & VAN DER VEEN, 1972).

A third function of the sand fill might be as a temporary storage reservoir for water that might flow into the cavity from some outside source.

At the end of each filling period, water must be removed from the injection well, the channel and the discharge well before gasification can be resumed. This can be done by introducing an inner tubing into one of the wells and depressing the liquid level with compressed air down to the shoe of this tubing. Hanging the tubing shoe near the bottom of the sand pack, as illustrated in figure 14, enables the pack to be emptied also. If gasification is carried out at a higher than hydrostatic pressure, and water collects in the sand pack, it can be continuously produced through the tubing.

The gas/liquid interface can be maintained at any desired level in the sand pack by manipulating the backpressure on the tubing.

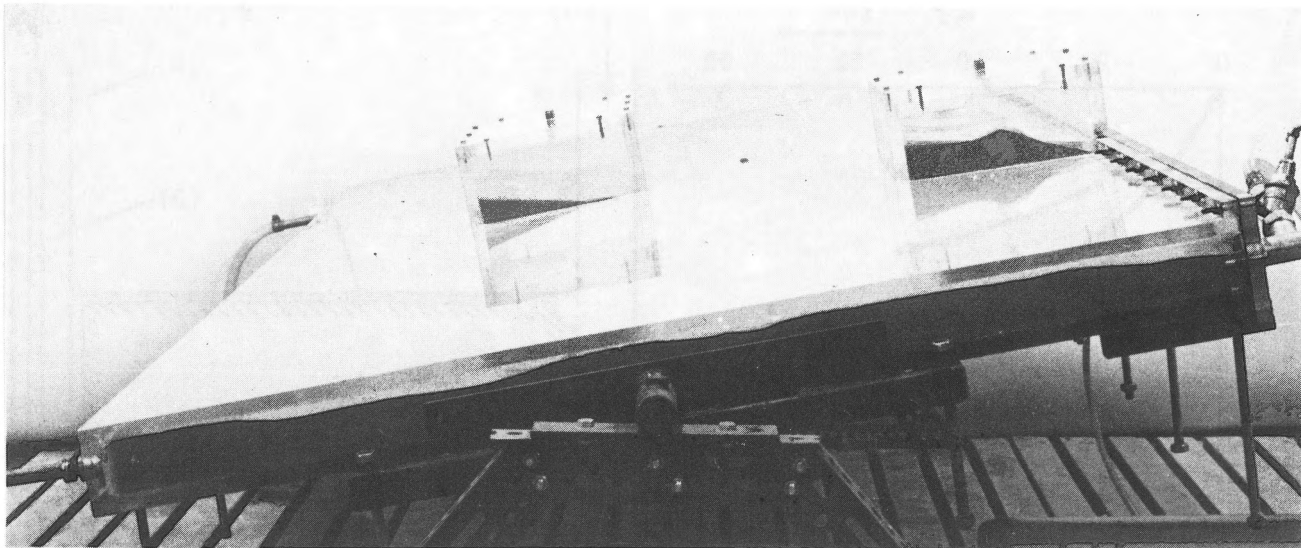


Fig. 15  
General view of the filled model with the two partly filled domes and the channel at the side of the model (protective frame removed).

Another interesting possibility is to partly evacuate the sand fill and subsequently introduce one or more chemical solutions to consolidate and strengthen it.

#### *Experiments with caved-in roof sections*

In longwall coal mining which is carried out at atmospheric pressure, the roof must be very thoroughly supported to prevent its caving-in. In underground gasification of coal it is not known if, and to what extent, roof collapse will occur. Not much can be learnt in this respect from experience gained in conventional coal mining, because the conditions are quite different. In the first place, the roof and floor rock will be exposed to high temperatures for extended periods of time. More important is perhaps that gasification will probably be carried out at high pressure. About the behaviour of deep cavities that are filled from time to time and are internally pressurized, nothing is known. It could be theorized that internal pressure, if continuously applied, might have a beneficial effect on the stability of such cavities (CHUGH & HARDY, 1972). As a result, caving-in of the roof might not occur at all during the application of internal pressure, or it might be less severe and more localized than is experienced in conventional longwall coal mining.

To determine, in a very general way, how the filling process would proceed with the roof locally caved-in, two box-shaped domes were built on top of the model, about halfway along its length. One dome is located updip near the front plate, the other one two-thirds of the way downdip (see Figs. 2 and 15). The dimensions are (length  $\times$  width  $\times$  height):  $23 \times 21 \times 8.5$  and  $29 \times 19 \times 8.5$  cm, which corresponds to field dimensions ( $n = 20$ ) of  $4.6 \times 4.2 \times 1.7$  m and  $5.8 \times 3.8 \times 1.7$  m respectively.

It was possible to fill the domes with water; to this end they

were provided with air valves.

Tests were carried out to find out if, and to what extent, the first dome would influence the development of the channel and if, and to what extent, both domes would influence the sedimentation process through the 'rivers' and the boundary layer. It was found that the domes had no influence at all on the filling process in the model, neither when filled with water, nor when filled with air. Around the domes the model fills up completely, whilst the domes themselves under both conditions partly fill up with sand.

The 'rivers' meander and turn updip underneath the domes as if these did not exist. When a 'river' is present under a dome that is filled with water, fluidisation of sand occurs in the dome as a result of which it partly fills up. The channel develops under the updip dome without being much influenced by it. Figure 16 shows a close-up of the sand fill in the updip dome, when filled with water.

To guarantee the continuity of the channel along the coal seam, it is advisable to wash out the fluidised sand from the

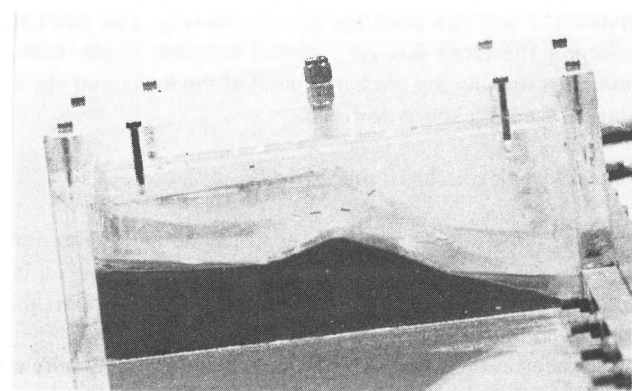


Fig. 16  
Close-up of the updip dome, filled with water and partly filled with sand.

updip dome by circulating with water. As was mentioned previously, this also increases the cross-section of the channel.

### CONCLUSIONS

Completely filling an underground cavity with sand is feasible. If the cavity is dipping, a channel develops updip along the coal seam. This channel can be enlarged by washing out with water. Localized caving-in of the roof does not hinder the filling process and the development of the channel; the filler will retain its supporting function.

Development of the channel, from which the cavity is filled, is a function of injection rate, grain size and dip angle of the cavity. Generally, injection rates can be chosen such that for a wide range of grain sizes filling is a stable process.

The cavity fills completely; the space that is left open at the end can be filled by positioning the discharge downdip. Probably this filling mechanism has taken place more than once in the past during sand invasions in coal mines.

### ACKNOWLEDGEMENTS

The authors wish to express their gratitude to Dr. A. K. Chesters of the Mechanical Engineering Faculty of Delft University for advice on the scaling rules and to the personnel of the workshop and the Sea Mining Laboratory of the

Mining Faculty for building the model and for technical assistance in carrying out the experiments. They are indebted to Mr. D. R. Horner for comments and suggestions on the English translation and to Mr. J. J. Swanink, Mrs. M. Vogelhaar and Mr. A. Steenhuis for the preparation of the figures, the manuscript and the photographs respectively.

The suggestions of the reviewers are gratefully acknowledged.

### REFERENCES

- Chugh, Y. P. & H. R. Hardy Jr. 1972 Analytical study of pressurized elliptical cavities – 14th Symp. Rock Mech., Pennstate Univ.
- De Groot, H. J. 1958 A water- and sand influx from the overburden into the mine Julia in Eyselshoven (in Dutch) – Geol. Mijnbouw N.S. 20: 421-429.
- Govier, G. W. & K. Aziz 1972 The flow of complex mixtures in pipes – Van Nostrand Reinhold Company (New York).
- Griffioen, A. & R. van der Veen 1972 Research and development in connection with tunnel foundation by using underflow with sand-water mixtures (in Dutch) – De Ingenieur 84: B77-B85.
- Gruppings, A. W. J. 1978 Underground gasification of coal with sand-fill (in Dutch) – De Ingenieur 90: 541-548.
- Sommer 1977 Die Überwindung eines Schwimmsandeinbruchs auf der Grube Sophia-Jacoba, Hüchelhoven – Glückauf 113: 533-539.
- Nesvacil, V. R. 1980 Multi-leg hole successfully drilled for degasification – Coal age 85: 140-150.
- Tyutin, F. G. 1958 The distribution and state of slag and packing material in the gasification void – Podz. Gazif. Uglei 2: 25-30 (Transl. P. R. Wilson, Humphreys & Glasgow Ltd.).
- Yalin, M. S. 1972 Mechanics of sediment transport – Pergamon Press (Oxford).